A Unified Model for Signal Transduction Reactions in Cellular Membranes

Jason M. Haugh
Department of Chemical Engineering, North Carolina State University, Raleigh, North Carolina 27695-7905 USA

ABSTRACT An analytical solution is obtained for the steady-state reaction rate of an intracellular enzyme, recruited to the plasma membrane by active receptors, acting upon a membrane-associated substrate. Influenced by physical and chemical effects, such interactions are encountered in numerous signal-transduction pathways. The generalized modeling framework is the first to combine reaction and diffusion limitations in enzyme action, the finite mean lifetime of receptor–enzyme complexes, reactions in the bulk membrane, and constitutive and receptor-mediated substrate insertion. The theory is compared with other analytical and numerical approaches, and it is used to model two different signaling pathway types. For two-state mechanisms, such as activation of the Ras GTPase, the diffusion-limited activation rate constant increases with enhanced substrate inactivation, dissociation of receptor–enzyme complexes, or crowding of neighboring complexes. The latter effect is only significant when nearly all of the substrate is in the activated state. For regulated supply and turnover pathways, such as phospholipase C-mediated lipid hydrolysis, an additional influence is receptor-mediated substrate delivery. When substrate consumption is rapid, this process significantly enhances the effective enzymatic rate constant, regardless of whether enzyme action is diffusion limited. Under these conditions, however, enhanced substrate delivery can result in a decrease in the average substrate concentration.

INTRODUCTION

The behavior of a living cell is dictated by its ability to integrate information about its changing environment, a complex biochemical process known as signal transduction. In animal cells, the plasma membrane plays a central role in organizing early signaling events, because it is accessible to intracellular and extracellular molecules. Indeed, signaling pathways are most often initiated by transmembrane receptors, which typically possess separate domains for engaging extracellular ligands and intracellular proteins. A well-characterized example is the class of receptor tyrosine kinases, which includes all growth factor receptors. Upon ligand binding and activation of their intrinsic tyrosine kinase domains, these receptors are autophosphorylated on multiple residues, which then participate in specific binding interactions with cytosolic enzymes (van der Geer et al., 1994; Pawson, 1995). The formation of such receptor–enzyme complexes is the first step in the activation of specific signaling pathways by receptor tyrosine kinases and many other signaling receptors.

When recruited by an activated receptor, a cytosolic protein is transiently confined within a thin layer adjacent to the plasma membrane. This leads to an interesting physical situation, because receptor-bound signaling enzymes often act upon specific lipid or lipid-anchored protein substrates that diffuse laterally in the membrane. For example, this is true of the three signaling cascades that have received the most attention over the past decade, the Ras, phospholipase C (PLC), and phosphoinositide (PI) 3-kinase pathways. Ras is a small GTPase most noted for its role in cell proliferation, which is inactive for signaling when bound to GDP and active when bound to GTP. It is anchored in the membrane by lipid modifications, and its nucleotide-binding state is regulated by cytosolic enzymes (Wittinghofer, 1998). PLC isoforms and type I PI 3-kinases are enzymes that modify a common lipid substrate, $PI(4,5)P_2$. PLC-mediated hydrolysis of $PI(4,5)P_2$ has varying functions in different cell types, including cell migration and gene expression, whereas phosphorylation of the lipid by PI 3-kinases has been implicated in chemotaxis and cell survival (Rhee and Bae, 1997; Rameh and Cantley, 1999). In each of these three major signaling pathways, recruitment of the relevant enzyme to the membrane is expected to have a significant impact on its observed activity. Indeed, enzymes isolated from lysates of stimulated cells often show little or no change in activity, whereas modifying these enzymes for stable membrane insertion is generally sufficient for activating downstream signaling in cells (Buday and Downward, 1993; Aronheim et al., 1994; Quilliam et al., 1994; Klippel et al., 1996).

The importance of enzyme localization in intracellular signaling suggests that significant insights could be gained through a combined biochemical and biophysical approach, whereby concentrations of membrane components, reaction-rate constants, and diffusion coefficients are quantitatively determined. The ability to accurately predict measured signaling pathway fluxes in cells would validate such an approach, but this would require an appropriate theoretical framework. In this paper, a generalized continuum model is formulated to describe various signaling pathways in which receptor–enzyme complexes modify laterally dif-

Submitted May 7, 2001 and accepted for publication October 24, 2001.

Address reprint requests to Jason M. Haugh, North Carolina State University, 113 Riddick Laboratories, Box 7905, Raleigh, NC 27695-7905. Tel.: 919-513-3851; Fax: 919-515-3465; E-mail: jason_haugh@ncsu.edu.

Abbreviations used: PLC, phospholipase C; PI, phosphoinositide; $PI(4,5)P_2$, phosphatidylinositol (4,5)-bisphosphate; MCT, mean capture time.

0006-3495/02/02/591/14 $2.00

fusing membrane substrates, with the primary goal of relating steady-state reaction rates to physical and kinetic constants.

The influence of translational diffusion on molecular interactions in two-dimensional (2D) domains has been the subject of numerous theoretical studies. With the mean capture time (MCT) approach, individual absorbers are placed at the centers of independent, circular domains, and molecules are reflected at the boundary to balance diffusion into and out of the domain (Adam and Delbrück, 1968; Berg and Purcell, 1977). Thus, the MCT approach introduces an ad hoc boundary condition and imposes that absorbers are evenly spaced, a nonrandom distribution. In contrast, the mean field (or effective medium) approximation smears absorbers throughout the domain, accounting for the depletion of molecules available to one absorber by each of the others (Wiegel and DeLisi, 1982; Goldstein et al., 1988; Khakhar and Agarwal, 1993). The problem of 2D diffusion in a random array of absorbers is mathematically analogous to the Brinkman equation describing fluid flow past an array of disks; for this system, it was found that the effective medium approximation is accurate for disk area fractions less than 0.3 (Howells, 1974; Dodd et al., 1995). Finally, an analysis of linearized statistical fluctuations about the average concentration has also been used to calculate diffusion-limited reaction rates (Keizer et al., 1985). Like the mean field approach, this theory allows the average concentration to be reached at infinite separation from an absorber.

Considering intracellular signaling interactions in particular, the effect of membrane localization on enzyme action has been estimated previously. Diffusion and reaction rate limitations have been considered simultaneously for both cytosolic and receptor-bound enzyme pools, using the MCT equation for the diffusion-limited contribution in the membrane (Haugh and Lauffenburger, 1997). A similar analysis considered that both pools experience either diffusion- or reaction-limited behavior, and the time-dependent diffusive flux to a single absorber in a semi-infinite membrane was used (Kholodenko et al., 2000). A different signaling mechanism, activation of heterotrimeric G proteins by direct interaction with ligated receptors, has been analyzed using Monte Carlo simulations on a 2D lattice (Mahama and Linderman, 1994). These simulations described, for the first time, how the average lifetime of receptor–ligand complexes can significantly affect steady-state G-protein activation rates in the diffusion limit. Indeed, Shea et al. (1997) used similar simulations to show that major discrepancies exist between effective rate constants obtained using Monte Carlo techniques and the various analytical approaches described above. However, the extent to which fundamental differences between lattice and continuum models affect the values of computed rate constants is unclear.

The results of the simulations performed by Linderman and colleagues reinforce the fact that the effective rate constant for a membrane reaction depends on all parameters that influence the substrate concentration profile in the membrane. The model presented here is therefore designed to be sufficiently general, including reactions that compete with, reverse the action of, or supply substrate to a receptor-recruited enzyme. Limitations imposed by diffusion and reaction on the action of this enzyme are considered simultaneously. Perhaps most importantly, it is demonstrated for the first time that a continuum approach can be used to describe receptor–enzyme complexes of finite average lifetime. Following the formulation of the general model, the implications of these various effects on the substrate concentration profile will be examined, with an emphasis on the Ras and PLC signaling pathways.

MATHEMATICAL MODEL FORMULATION

Model considerations

To construct a realistic model with as few adjustable parameters as possible, three major assumptions are invoked:

1. There is a random distribution of cell surface receptors active for signaling within the membrane domain of interest. Although certainly reasonable as a default assumption, the theory may not be accurate in certain regions of the membrane, such as near clathrin-coated pits when internalization of receptors is diffusion-limited (Goldstein et al., 1988).
2. The enzymatic reaction in the membrane follows a second-order rate law, with a rate proportional to the concentrations of substrate and receptor–enzyme complexes in the membrane. Thus, in terms of Michaelis–Menten kinetics, the Michaelis constant K_M is significantly greater than the membrane concentrations of either species. The resulting second-order rate constant is given by the k_{cat}/K_M ratio of the enzyme at the membrane, where k_{cat} is the first-order catalytic rate constant.
3. The mobility of substrate molecules relative to receptor–enzyme complexes is described by 2D Fickian diffusion in a semi-infinite domain, with a constant diffusion coefficient. In making this assumption, nonidealities associated with diffusion in cellular membranes, and complex media in general, must be acknowledged (Sheetz, 1993; Feder et al., 1996; Pralle et al., 2000). However, the motion of the lipid or lipid-anchored substrate is expected to dominate the diffusion coefficient in this case. Unlike many transmembrane receptors, such molecules exhibit diffusion coefficients close to theoretical values and essentially complete fluorescence recovery after photobleaching (Schlessinger et al., 1977; Niv et al., 1999).

In the sections that follow, models describing two distinct signaling-pathway types will be presented (Fig. 1). Major signaling pathways adequately simulated by each model are discussed, and the appropriate equations are formulated. It is then shown that a generalized model encompasses both pathway types, and analytical solutions are derived for the effective enzymatic rate constant at steady state. Finally, the theory is extended to account for the finite mean lifetime of receptor–enzyme complexes.

Pathway type 1: reversible, two-state mechanism

In signaling pathways of this type (Fig. 1 *a*), a membrane-associated substrate is converted to an activated state by a receptor-recruited enzyme. The inactive substrate is later recovered by a first-order reaction, such that the total number of molecules in the active and inactive states is conserved on the time scale of interest. Regulation of the membrane-anchored GTPase Ras, which is inactive in the GDP-bound state and active in the

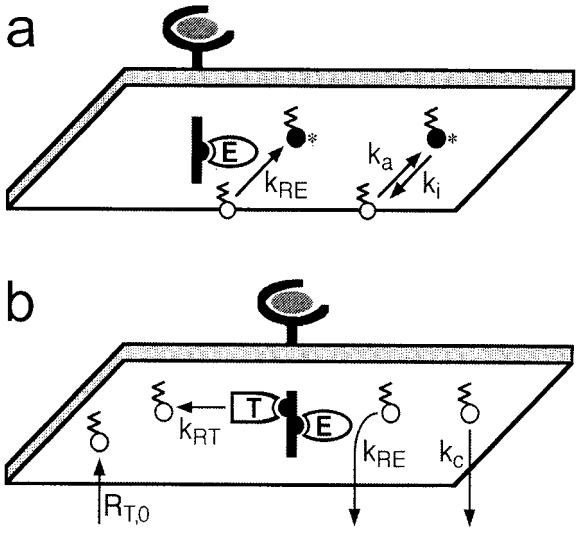

FIGURE 1 Pathway types described by the general model. (*a*) Two-state mechanism. A membrane-anchored substrate is converted back and forth between inactive and activated states. Activation and inactivation occur in the bulk membrane with observed first-order rate constants k_a and k_i, respectively. Substrate activation is enhanced by receptor–enzyme complexes, which act upon inactive substrate with second-order rate constant k_{RE}. (*b*) Regulated supply and turnover. The concentration of a membrane-anchored substrate is determined by the relative rates of consumption and transfer to the membrane. The first-order rate constant describing basal consumption is k_c, and $R_{T,0}$ is the basal rate of substrate transfer. Both the turnover and supply of the substrate are modulated by activated receptors. Receptor–enzyme complexes consume substrate with second-order rate constant k_{RE}, whereas receptor–transfer protein complexes deliver substrate with first-order rate constant k_{RT}.

GTP-bound state, is well described by this two-state model. In numerous cell types, an increase in Ras-GTP is mediated by the recruitment of guanine nucleotide exchange factors (GEFs) from the cytosol to the plasma membrane, in complex with adaptor proteins that link them to signaling receptors (Medema et al., 1993; Buday and Downward, 1993). GEFs catalyze the dissociation of bound nucleotides from Ras in cells; the subsequent rebinding of nucleotides is extremely rapid, favoring uptake of the more abundant GTP (Lenzen et al., 1998). To recover Ras-GDP, the GTPase activity of Ras hydrolyzes bound GTP, a reaction that is significantly accelerated by GTPase-activating proteins (GAPs). These GAP activities help maintain the majority of Ras in the GDP-bound state prior to cell stimulation (Wittinghofer et al., 1997). The two-state mechanism also serves as an idealized model of G-protein activation. Ligand-bound G protein-coupled receptors interact directly with heterotrimeric G proteins, which are composed of α, β, and γ subunits (Hamm and Gilchrist, 1996). The GDP-bound α subunit is thereby converted to the active GTP-bound state and liberated from the $\beta\gamma$ subunits; following the GTPase reaction and recovery of the GDP-bound state, the α and $\beta\gamma$ subunits rapidly reassociate.

In this model pathway, substrate in the inactive state is conserved by

$$\frac{\partial n_S}{\partial t} = D\nabla_r^2 n_S - (k_a + k_{RE}^{eff} n_{RE}) n_S + k_i n_{S*}, \qquad (1)$$

where n_S is the 2D concentration of the inactive substrate as a function of radial distance r from a receptor–enzyme complex and time t. The lateral diffusion coefficient of the substrate relative to receptor–enzyme complexes, D, is assumed to have the same value for the inactive and active states. The first-order rate constants k_a and k_i characterize constitutive activation and inactivation steps, respectively; the latter acts upon the active form of the substrate, which has a 2D concentration n_{S*}. The mean field approximation is introduced through the inclusion of a rate term that accounts for consumption of substrate by each of the neighboring receptor–enzyme complexes (2D concentration n_{RE}), with effective second-order rate constant k_{RE}^{eff}. Substituting the relation $n_S + n_{S*} = n_{S,tot}$ = constant, one finds that

$$\frac{\partial n_S}{\partial t} = D\nabla_r^2 n_S - (k_a + k_i + k_{RE}^{eff} n_{RE}) n_S + k_i n_{S,tot}. \qquad (2)$$

Eq. 2 is subject to two boundary conditions. At the enzyme–substrate encounter distance ($r = s$, interpreted as the sum of the associating molecules' radii), the flux of inactive substrate to each receptor–enzyme complex is balanced by the rate of the enzymatic reaction. The true second-order rate constant of the reaction is k_{RE}. The second boundary condition maintains a finite value of n_S at infinite separation from the receptor–enzyme complex; this value of n_S is equivalent to its average in the membrane, defined as $\bar{n}_S$,

$$2\pi s D \left.\frac{\partial n_S}{\partial r}\right|_{r=s} = k_{RE} n_S|_{r=s}; \qquad n_S|_{r=\infty} \equiv \bar{n}_S. \qquad (3)$$

Finally, the enzymatic reaction rate, k_{RE}^{eff}, and k_{RE} are related by

$$\text{rate} = k_{RE}^{eff} n_{RE} \bar{n}_S = k_{RE} n_{RE} n_S|_{r=s}. \qquad (4)$$

It follows that the effective rate constant k_{RE}^{eff} deviates from k_{RE} when the substrate is not homogeneously distributed, and so the magnitude of k_{RE}^{eff} can be used to assess the influence of spatial effects on the reaction rate.

Pathway type 2: regulated substrate supply and turnover

In signaling pathways of this type (Fig. 1 *b*), a membrane-associated substrate is consumed by receptor–enzyme complexes, but here the action of the enzyme cannot be reversed by another reaction in the membrane. Rather, the substrate is delivered to the membrane continuously by a cytosolic transfer protein. Like the enzyme, a fraction of the transfer protein is engaged by activated receptors, and it is assumed that the enzyme and transfer protein bind to independent receptor sites. The formation of receptor–transfer protein complexes enhances substrate delivery, allowing higher reaction rates through the receptor–enzyme complexes, and the availability of substrate is determined by the relative extents to which its supply and consumption are modulated.

The action of receptor-recruited PLC, which hydrolyzes the membrane lipid PI(4,5)P_2, is well described by this model. The products of PI(4,5)P_2 hydrolysis are inositol (1,4,5)-trisphosphate, released into the cytosol, and (1,2)-diacylglycerol, which remains in the membrane. These products are metabolized and then recombined to form phosphatidylinositol in the endoplasmic reticulum, and this lipid precursor must be transferred to the plasma membrane for reconstitution of the substrate PI(4,5)P_2 (Hsuan and Tan, 1997; Toker, 1998). To prevent depletion of PI(4,5)P_2, its supply to the plasma membrane is also positively modulated by receptor stimulation (Batty et al., 1998; Willars et al., 1998). The PI(4,5)P_2 delivery rate is probably influenced by direct interactions between receptors and proteins involved in phosphatidylinositol transfer and phosphorylation (Kauffmann-Zeh et al., 1994, 1995). The regulated supply and turnover model is also suitable for the PI 3-kinase pathway, in which PI(4,5)P_2 is phosphorylated to form the lipid second messenger PI(3,4,5)P_3 (Vanhaesebroeck and Waterfield, 1999). Though this reaction can be reversed in the membrane by different routes, the action of PI 3-kinase is expected to be influenced by the aforementioned regulation of the PI(4,5)P_2 concentration.

TABLE 1 Dimensionless model parameters

Parameter	Definition*		Brief description	Estimated range†
	Two-state	Regulated Supply		
κ		k_{RE}/D	Enzyme reaction rate constant	10^{-3}–10^{3}
η_R		$s^2 n_R$	Activated receptor density	10^{-8}–10^{-1}
η_{RE}		$s^2 n_{RE}$	Receptor-enzyme density	10^{-8}–10^{-1}
τ_{RE}		Dt_{RE}/s^2	Receptor-enzyme lifetime	10–10^{7}
Da	$(k_a+k_i)s^2/D$	$k_c s^2/D$	Bulk membrane rate constant	10^{-7}–10^{-1}
β	0	$(n_{RT}/n_R)\ k_{RT}/s^2 R_{T,0}$	Enhancement of substrate supply	No estimate

*See Fig. 1 for illustrations of the various rate processes.
†Parameter ranges are calculated as follows: k_{RE} is estimated using a k_{cat}/K_M range of 10^4–10^8 $(Ms)^{-1}$ and dividing by a confinement layer of ~3–10 nm; n_R and n_{RE} are estimated as 1–10^6 molecules in a 10^3-μm^2 membrane; the rate constants k_i, k_c, and t_{RE}^{-1} are given a range spanning 0.01–100 s^{-1}; other estimates are $s \sim$ 3–10 nm, D ~ 0.1–1 $\mu m^2/s$.

The substrate conservation equation for the regulated supply and turnover model is

$$\frac{\partial n_S}{\partial t} = D\nabla_r^2 n_S - (k_c + k_{RE}^{eff} n_{RE}) n_S + R_{T,0} + k_{RT} n_{RT}. \quad (5)$$

Again, $n_S(r, t)$ and D are the concentration and relative diffusion coefficient of the substrate, n_{RE} is the concentration of receptor–enzyme complexes, and k_{RE}^{eff} is the effective second-order rate constant for enzyme action at the membrane. The first-order rate constant k_c describes basal substrate consumption, and $R_{T,0}$ is the basal rate of substrate delivery to the membrane. Substrate delivery is accelerated by receptor–transfer protein complexes (2D concentration n_{RT}), which insert substrate with first-order rate constant k_{RT}. The boundary condition at the enzyme–substrate encounter distance ($r = s$) is given by

$$2\pi s D \left.\frac{\partial n_S}{\partial r}\right|_{r=s} = k_{RE} n_S|_{r=s} - \left(\frac{n_{RT}}{n_R}\right) k_{RT}, \quad (6)$$

where k_{RE} is the second-order rate constant of the enzymatic reaction. The second term on the right-hand side of Eq. 6 accounts for the possibility that the receptor engaging the enzyme may be bound to a transfer protein as well, in which case substrate will be delivered at this location. This probability is given by n_{RT}/n_R, where n_R is the total concentration of activated receptors in the membrane. The boundary condition at $r = \infty$ and the relationship between k_{RE}^{eff} and k_{RE} are the same as in the two-state model.

General model and solution for stable receptor–enzyme complexes

A conservation equation and encounter-distance boundary condition that encompass both of the pathway models illustrated in Fig. 1 can be posed,

$$\frac{\partial n_S}{\partial t} = D\nabla_r^2 n_S - (k_0 + k_{RE}^{eff} n_{RE}) n_S + V_0 + k_v n_R,$$

$$2\pi s D \left.\frac{\partial n_S}{\partial r}\right|_{r=s} = k_{RE} n_S|_{r=s} - k_v. \quad (7)$$

Here, the identities of the rate constants k_0 and k_v and the source term V_0 will depend on the pathway type. In the two-state model, $k_0 \equiv k_a + k_i$, $V_0 \equiv k_i n_{S,tot}$, and $k_v = 0$; in the regulated supply and turnover model, $k_0 \equiv k_c$, $V_0 \equiv R_{T,0}$, and $k_v \equiv (n_{RT}/n_R)k_{RT}$. To reduce the number of constant parameters, Eq. 7 is nondimensionalized,

$$\frac{\partial \Psi}{\partial \tau} = \nabla_\rho^2 \Psi - (Da + \alpha\eta_{RE})\Psi + 1 + \beta\eta_R;$$

$$2\pi \left.\frac{\partial \Psi}{\partial \rho}\right|_{\rho=1} = \kappa\Psi|_{\rho=1} - \beta;$$

$$\Psi \equiv \frac{D n_S}{s^2 V_0}; \quad \tau \equiv \frac{Dt}{s^2}; \quad \rho \equiv \frac{r}{s}; \eta_R \equiv s^2 n_R; \quad \eta_{RE} \equiv s^2 n_{RE};$$

$$Da \equiv \frac{s^2 k_0}{D}; \quad \alpha \equiv \frac{k_{RE}^{eff}}{D}; \ \beta \equiv \frac{k_v}{s^2 V_0}; \quad \kappa \equiv \frac{k_{RE}}{D}. \quad (8)$$

The dimensionless parameter Da is a Damköhler number comparing the rates of basal consumption and diffusion of the substrate. The effective and actual second-order enzymatic rate constants are scaled to the diffusion coefficient D to yield α and κ, respectively. The dimensionless density of activated receptors is given by η_R, and η_{RE} is the corresponding density of activated receptors bound to enzyme. The enhancement of the substrate delivery rate by activated receptors is characterized by β. The identities of these dimensionless parameters and their estimated value ranges are summarized in Table 1.

When the lifetime of a receptor–enzyme complex is much longer than the time required for the substrate profile to evolve around it, the following steady state solution is obtained:

$$\Psi_{ss}(\rho) = \bar{\Psi}_{ss} - \frac{(\kappa\bar{\Psi}_{ss} - \beta)K_0(Da^{*1/2}\rho)}{2\pi Da^{*1/2}K_1(Da^{*1/2}) + \kappa K_0(Da^{*1/2})};$$

$$\bar{\Psi}_{ss} = \frac{1 + \beta\eta_R}{Da^*}; \quad Da^* \equiv Da + \alpha\eta_{RE}, \quad (9)$$

where K_i are modified Bessel functions of order i, and $\bar{\Psi}_{ss}$ is the dimensionless analog of $\bar{n}_S$ at steady state. Finally, an implicit solution relating the steady-state effective rate constant α to the other parameters is found,

$$\alpha = \kappa \frac{\Psi_{ss}(1)}{\bar{\Psi}_{ss}} = \frac{\kappa[2\pi f(Da^{*1/2}) + \beta Da^*/(1 + \beta\eta_R)]}{\kappa + 2\pi f(Da^{*1/2})};$$

$$f(x) \equiv x\frac{K_1(x)}{K_0(x)}. \quad (10)$$

A possible modification of Eq. 8 is to distinguish receptor–enzyme complexes that are contributing to substrate delivery from those that are not with separate boundary conditions. It was confirmed that such an approach, with an overall α computed as a weighted sum of the α values for the two receptor pools, yields the same result as in Eq. 10 (not shown).

At this stage, it is instructive to review limiting cases of Eq. 10 and compare these with previous analytical theories. In the limit of low receptor–enzyme density, the term in Eq. 8 invoking the mean field approximation vanishes, and Eq. 10 becomes an explicit function of constant parameters (Da* = Da). For the case of $\beta = 0$, this low-density limit was derived previously to describe the Langmuir–Hinshelwood surface reaction mechanism with reactant absorption/desorption (Freeman and Doll, 1983). In the limit of very high receptor–enzyme density (Da* $\gg$ Da) and $\beta = 0$, the result of Wiegel and DeLisi (1982) describing binding of ligands to cell receptors through nonspecific membrane adsorption and diffusion is obtained. The effective rate constant at any receptor–enzyme density, again with $\beta = 0$, also agrees with results derived for other systems. Goldstein et al. (1988) described diffusion-limited capture of cell surface receptors by internalizing traps, and Khakhar and Agarwal (1993) extended the work of Freeman and Doll to describe the Langmuir–Hinshelwood mechanism for higher reactant densities.

General model solution for receptor–enzyme complexes with finite mean lifetime

In general, an individual enzyme–receptor complex may dissociate before the substrate concentration can achieve the profile predicted from Eq. 9, though a constant concentration of such complexes will be maintained, on average, at steady state. Hence, the mean field approach was used to calculate the impact of receptor–enzyme complex stability on the effective enzymatic rate constant. It should be noted that the receptor-dependent source term, characterized by β, might involve a receptor–transfer protein complex; this interaction is assumed to be stable, because its lifetime is not considered here.

Eq. 8 is used to derive the evolution of the substrate concentration profile surrounding an individual enzyme–receptor complex during its lifetime (the "enzyme-on" phase), with the average density of receptor–enzyme complexes at steady state reflected in the effective rate term. The transient solution is given by

$$\Psi(\rho, \tau) = \Psi_{ss}(\rho) + \int_0^\infty \left[\Theta(0) + \frac{(\kappa\bar{\Psi}_{ss} - \beta)\Phi(1)}{2\pi(\lambda^2 + \mathrm{Da}^*)}\right] \times \left[\frac{\Phi(\rho)e^{-(\lambda^2+\mathrm{Da}^*)\tau}}{1 + g^2(\lambda)}\right]\lambda\, d\lambda;$$

$$\Phi(\rho) \equiv J_0(\lambda\rho) - g(\lambda)Y_0(\lambda\rho);$$

$$g(\lambda) \equiv \frac{\kappa J_0(\lambda) + 2\pi\lambda J_1(\lambda)}{\kappa Y_0(\lambda) + 2\pi\lambda Y_1(\lambda)};$$

$$\Theta(0) \equiv \int_1^\infty [\Psi(\rho, 0) - \bar{\Psi}_{ss}]\Phi(\rho)\rho\, d\rho, \qquad (11)$$

where $\Psi_{ss}(\rho)$ is the steady-state substrate profile in the infinite lifetime limit (Eq. 9), $\Psi(\rho, 0)$ is the initial substrate profile, and J_i and Y_i are Bessel functions of order i. Eq. 11 is obtained using either Fourier-like integral transform or Laplace transform (Carslaw and Jaeger, 1940) solution methods. The dimensionless mean lifetime of the complex, inversely proportional to the dissociation rate constant of the receptor–enzyme interaction, is defined as τ_{RE}. The effective enzymatic rate constant is then found using the implicit relation,

$$\alpha = \kappa\frac{\int_0^{\tau_{RE}}\Psi(1, \tau)d\tau}{\bar{\Psi}_{ss}\tau_{RE}}. \qquad (12)$$

After the complex dissociates, the substrate profile around the free activated receptor homogenizes. The transient for this "enzyme-off" phase is found by analogy to Eq. 11, with $\kappa = 0$. The initial condition is given by the substrate profile at the end of the enzyme-on phase, calculated from Eq. 11. The dimensionless average duration of the enzyme-off state is defined as τ_R, and

$$\tau_R = \left(\frac{\eta_R}{\eta_{RE}} - 1\right)\tau_{RE}. \qquad (13)$$

This process is important because the substrate profile at the end of the enzyme-off phase is the initial condition for the next enzyme-on phase, and so on. This implicit condition is required to completely specify the problem, but the solution simplifies greatly for the interesting limiting cases. As τ_R vanishes ($\eta_{RE}/\eta_R \approx 1$), it is readily shown that $\Psi = \Psi_{ss}$; the finite complex lifetime does not matter, because the cytosolic concentration of the enzyme is high enough to saturate all activated receptors. As τ_R becomes large ($\eta_{RE}/\eta_R \ll 1$), it is apparent that $\Psi(\rho, 0) = \bar{\Psi}_{ss}$ at the beginning of each enzyme-on phase, and the implicit relation for the effective enzymatic rate constant becomes

$$\alpha = \kappa\frac{\Psi_{ss}(1)}{\bar{\Psi}_{ss}} + \frac{8}{\pi\tau_{RE}}\left[1 - \frac{\beta\mathrm{Da}^*}{\kappa(1 + \beta\eta_R)}\right] \times \int_0^\infty \frac{[1 - e^{-(\lambda^2+\mathrm{Da}^*)\tau_{RE}}](\lambda^2 + \mathrm{Da}^*)^{-2}\lambda\, d\lambda}{\left[\frac{J_0(\lambda) + 2\pi\lambda J_1(\lambda)}{\kappa}\right]^2 + \left[\frac{Y_0(\lambda) + 2\pi\lambda Y_1(\lambda)}{\kappa}\right]^2}. \qquad (14)$$

Eq. 14 was obtained from Eq. 12 by specifying the initial condition as the homogeneous $\bar{\Psi}_{ss}$ and evaluating $\Psi(1, \tau)$ from Eq. 11. The integral is evaluated numerically. In the purely diffusion-limited regime ($\kappa \to \infty$), Eq. 14 further simplifies to

$$\alpha = 2\pi\mathrm{Da}^{*1/2}\frac{K_1(\mathrm{Da}^{*1/2})}{K_0(\mathrm{Da}^{*1/2})} + \frac{\beta\mathrm{Da}^*}{1 + \beta\eta_R} + \frac{8}{\pi\tau_{RE}}\int_0^\infty \frac{[1 - e^{-(\lambda^2+\mathrm{Da}^*)\tau_{RE}}]\lambda\, d\lambda}{(\lambda^2 + \mathrm{Da}^*)^2[J_0^2(\lambda) + Y_0^2(\lambda)]}. \qquad (15)$$

A satisfying result is the presence of three clearly separated contributions to the effective rate constant in this regime. The first term describes a receptor–enzyme complex of infinite lifetime, the second describes the contribution of receptor-mediated substrate delivery (nonzero β), and the third contains the influence of a finite lifetime τ_{RE}.

RESULTS AND DISCUSSION

Two-state mechanism

Influences of substrate inactivation and neighboring receptor–enzyme complexes on the effective enzymatic rate constant

The major difference between the two pathway types illustrated in Fig. 1 is the nature of the receptor-mediated sub-

strate delivery term, characterized by the dimensionless parameter β. In pathway type 1 (Fig. 1 *a*), a two-state mechanism appropriate for modeling activation of small GTPases such as Ras, $\beta = 0$. Another difference is the definition of the Damköhler number Da. In the two-state mechanism, Da reflects the sum of the basal activation and inactivation rate constants (k_a and k_i, respectively). Pathways of this type typically exhibit low levels of activation in the absence of receptor stimulation, and $k_i \gg k_a$ when this is the case. Indeed, with $k_a = 0$ and diffusion-controlled enzyme action ($\kappa \to \infty$), pathway type 1 is indistinguishable from the collision coupling mechanism (Tolkovsky and Levitski, 1978). Thus, the value of Da generally describes how rapidly the activated substrate molecules are inactivated as they diffuse away from receptor–enzyme complexes.

The model formulation allows reaction and diffusion limitations in the action of receptor–enzyme complexes to be considered simultaneously. In Fig. 2 *a*, the effective enzymatic rate constant, α, is plotted versus the true reaction rate constant, κ, for various values of Da; here, receptor–enzyme complexes are sparse but highly stable ($\eta_{RE} \to 0$, $\tau_{RE} \to \infty$). With $\kappa \ll 1$, the action of the enzyme is expected to be reaction-limited, with minimal depletion of inactive substrate at the encounter distance $r = s$. As expected, $\alpha \approx \kappa$ in this limit. With $\kappa \gg 1$, the action of the enzyme is limited by the translational diffusion of the substrate, at the same time that the enzyme depletes the majority of the inactivated substrate molecules in its vicinity. The value of α is insensitive to κ and positively dependent on Da in this limit (Fig. 2 *a*). The gradient of inactivated substrate at the encounter distance gets larger as Da increases, because the inactivation process replenishes the substrate of the enzyme. The influence of the inactivation process on the diffusion-limited value of α in the low-density, stable-complex limit has also been derived using a different approach (Molski, 2000). The diffusion-limited value of α becomes sensitive to Da when the time scale of substrate inactivation is comparable to s^2/D (Da $\sim$ 1). For typical membrane substrates, $s^2/D < 1$ ms, faster than most unsaturated enzymes can process substrate. Therefore, the diffusion-limited value of the effective activation-rate constant α is expected to fall within a relatively narrow range of 0.7–2.5 for stable receptor–enzyme complexes at low density.

The theory can also predict the diffusion-limited enzymatic rate constant at relatively high densities of receptor–enzyme complexes, an effect incorporated using the mean field approach. This is illustrated in Fig. 2 *b*, in which the effective enzymatic rate constant α is plotted versus the receptor–enzyme density η_{RE} for various Da in the diffusion-limited, stable-complex limit ($\kappa \to \infty$, $\tau_{RE} \to \infty$). As values at the high end of the estimated η_{RE} range are approached, α increases above the low density limit and becomes insensitive to the value of Da. In the high-density regime, neighboring receptor–enzyme complexes interfere

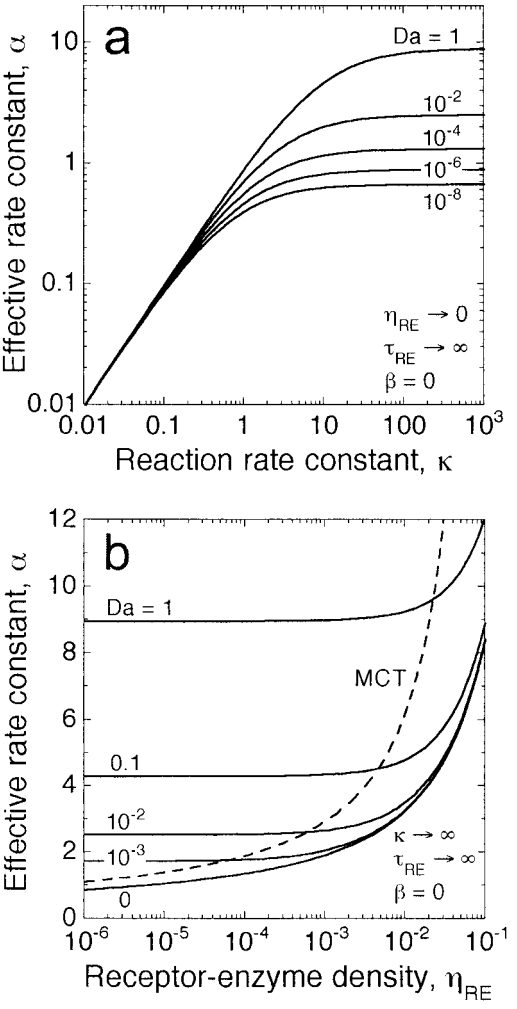

FIGURE 2 Effective enzymatic rate constant, two-state mechanism: stable receptor–enzyme complexes. (*a*) The effective rate constant α is computed as a function of the dimensionless rate constant $\kappa = k_{RE}/D$, for the indicated values of Da = $(k_a + k_i)s^2/D$ and stable receptor-enzyme complexes at low density ($\eta_{RE} \to 0$, $\tau_{RE} \to \infty$). (*b*) The effective rate constant α is computed as a function of the dimensionless receptor-enzyme density $\eta_{RE} = s^2 n_{RE}$ for the indicated values of Da, diffusion-limited enzyme action, and stable receptor–enzyme complexes ($\kappa \to \infty$, $\tau_{RE} \to \infty$). The dashed line is the prediction of the MCT approach (Eq. 16).

with the substrate concentration profile surrounding each complex; substrate activation dominates over the inactivation process ($\alpha\eta_{RE} >$ Da), and the inactive substrate profile becomes more homogeneous. Hence, the diffusion-limited value of the effective rate constant α increases. Also plotted in Fig. 2 *b* is the prediction of the MCT approach (Berg and Purcell, 1977),

$$\alpha_{MCT} = 2\pi\left\{\ln\left[\frac{1}{(\pi\eta_{RE})^{1/2}}\right] - \frac{(3 - \pi\eta_{RE})(1 - \pi\eta_{RE})}{4}\right\}^{-1}. \quad (16)$$

In this form, the MCT equation accounts for diffusion between evenly spaced activating enzymes but does not

include the inactivation process. However, even when Da = 0, Fig. 2 *b* shows that the organization of receptor–enzyme complexes in regularly spaced domains yields noticeable deviations from the mean field approach, which considers a random distribution of complexes.

Influence of receptor–enzyme complex lifetime on the enzymatic rate constant and comparison with Monte Carlo simulations

By solving for the transient substrate profile surrounding an average receptor–enzyme complex, the theory was extended to incorporate the kinetics of complex association and dissociation. Based on the results of Monte Carlo simulations, a short-lived receptor–enzyme pair is not expected to disturb the initially homogeneous substrate distribution as drastically as a stable complex would (Shea et al., 1997). This yields a sharper substrate gradient, averaged over the lifetime of the complex. Analytical theories, which heretofore have not accounted for these effects, therefore tend to underestimate the activation rate constant when the lifetime of the enzyme at the membrane is relatively short.

The influence of the dimensionless receptor–enzyme complex lifetime, τ_{RE}, on the effective rate constant α for the two-state mechanism is shown in Fig. 3. In Fig. 3 *a*, α is plotted versus τ_{RE} for various values of Da and a vanishing density of receptor–enzyme complexes in the diffusion limit ($\kappa \to \infty$, $\eta_{RE} \to 0$). In accord with the Monte Carlo study cited above, α is a decreasing function of the receptor–enzyme-complex lifetime for very low values of τ_{RE}, and this trend is independent of Da. However, as τ_{RE} is increased above Da^{-1}, α approaches the stable-complex limit, which is solely dependent on the value of Da (Fig. 3 *a*). The latter effect was not described in the Monte Carlo simulation study, because the Da values used were less than 10^{-3} and never exceeded τ_{RE}^{-1}. Hence, the conclusion that the effective rate constant scales with $4Dt_{RE}$, the mean-squared displacement of substrate during the lifetime of the active complex (Shea et al., 1997), needs to be qualified. At low receptor–enzyme densities, the value of α is determined by the fastest process that limits the spread of active substrate molecules in the membrane, either receptor–enzyme dissociation or substrate inactivation. A quantitative comparison of effective rate constant values obtained using the general model and Monte Carlo simulations is explored in the Appendix.

Figure 3 *b* shows the effect of increasing the density of receptor–enzyme complexes, η_{RE}, on the diffusion-limited effective rate constant when the mean lifetime of these complexes is finite. For all values of η_{RE}, it is assumed that few activated receptors are in complex with enzyme molecules ($\eta_{RE} \ll \eta_R$; Eq. 13), such that Eq. 15 can be used to compute α. The effective rate constant α is shown to be a positive function of the receptor–enzyme density, and this trend becomes independent of the receptor–enzyme lifetime as η_{RE} increases (Fig. 3 *b*). Indeed, it is apparent that the effects of a finite lifetime, when $\tau_{RE}^{-1} \gg$ Da (Fig. 3 *b*), and the inactivation process, when Da $\gg \tau_{RE}^{-1}$ (Fig. 2 *b*), show similar behavior across the spectrum of receptor–enzyme density values. Taken together, the results shown in Figs. 2 and 3 demonstrate that any one of three processes can limit the spread of the inactivated substrate gradient surrounding each receptor–enzyme complex and set the value of the effective enzymatic rate constant. These include substrate inactivation, characterized by Da, receptor–enzyme complex dissociation, characterized by τ_{RE}^{-1}, and the action of neighboring receptor–enzyme complexes, characterized by η_{RE}.

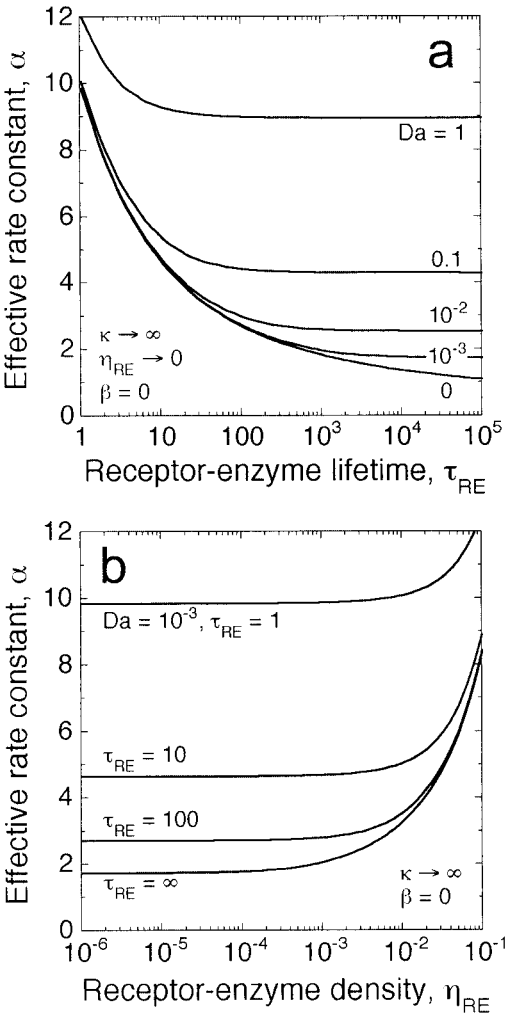

FIGURE 3 Effective enzymatic rate constant, two-state mechanism: receptor–enzyme complexes with finite mean lifetime. (*a*) The effective rate constant α is computed as a function of the dimensionless receptor–enzyme lifetime $\tau_{RE} = Dt_{RE}/s^2$ for the indicated values of Da, diffusion-limited enzyme action, and receptor–enzyme complexes at low density ($\kappa \to \infty$, $\eta_{RE} \to 0$). (*b*) The effective rate constant α is computed as a function of the dimensionless receptor-enzyme density η_{RE} for the indicated values of τ_{RE}, Da = 10^{-3}, $\eta_{RE}/\eta_R \ll 1$, and diffusion-limited enzyme action ($\kappa \to \infty$).

Predicting the fraction of substrate in the activated state

With steady or pseudo-steady state signaling through the two-state mechanism, the fraction of substrate in the activated state is given by

$$\frac{\bar{n}_{S^*}}{n_{S,tot}} = \frac{k_a + k_{RE}^{eff} n_{RE}}{k_a + k_i + k_{RE}^{eff} n_{RE}} = \frac{\frac{K_a S^2}{D} + \alpha \eta_{RE}}{Da + \alpha \eta_{RE}}. \quad (17)$$

One of the interesting features of the mean field model, as well as the MCT equation (Eq. 16), is that the effective rate constant α is a function of the receptor–enzyme density η_{RE} in the diffusion limit (Figs. 2 *b* and 3 *b*). This offers the possibility that the activated substrate fraction, given by Eq. 17, is a complex function of η_{RE}. This possibility is explored in Fig. 4, in which the activated substrate fraction is plotted versus the receptor–enzyme density η_{RE} with $k_a = 0$ and diffusion-limited enzyme action (equivalent to the collision coupling mechanism).

In Fig. 4 *a*, complexes are long-lived ($\tau_{RE} \to \infty$), and substrate activation curves are plotted for various values of Da. Also shown in Fig. 4 *a* are the corresponding activation curves computed using the constant, low-density limit of α. For the values of Da shown, the constant α curves underestimate the exact values when activated substrate fractions exceed 0.2, with a maximum deviation of 5–10% seen at activated substrate fractions of 0.8–0.9. Neglecting the action of neighboring receptor–enzyme complexes therefore introduces a minor but noticeable error. The error is mitigated by the fact that the strong dependence of α on η_{RE} occurs in a regime of nearly complete substrate activation ($\alpha\eta_{RE} \gg$ Da; see Eq. 17). Finally, activation curves using the MCT equation for α (Eq. 16) are also plotted for comparison in Fig. 4 *a*. In this case, the deviations are significant, particularly at high Da values. Substrate activation is underpredicted at low η_{RE} and overpredicted at high η_{RE}.

The impact of decreasing the mean receptor–enzyme complex lifetime, τ_{RE}, is shown in Fig. 4 *b*. Based on the analysis of Fig. 3, it was concluded that a reduction in τ_{RE} has a similar effect on α as an increase in Da, for the same value of η_{RE}. With respect to the level of activated substrate, however, a decrease in τ_{RE} shifts the activation curve to the left (Fig. 4 *b*), in qualitative contrast with the effect of a Da increase. The value of η_{RE} that elicits half-maximal substrate activation is given by Da/α, and, unlike an increase in Da, a reduction in τ_{RE} increases only the denominator in this ratio. In agreement with Monte Carlo results (Mahama and Linderman, 1994), neglecting receptor–enzyme dissociation can lead to a significant overestimate of the receptor–enzyme density required for half-maximal signaling.

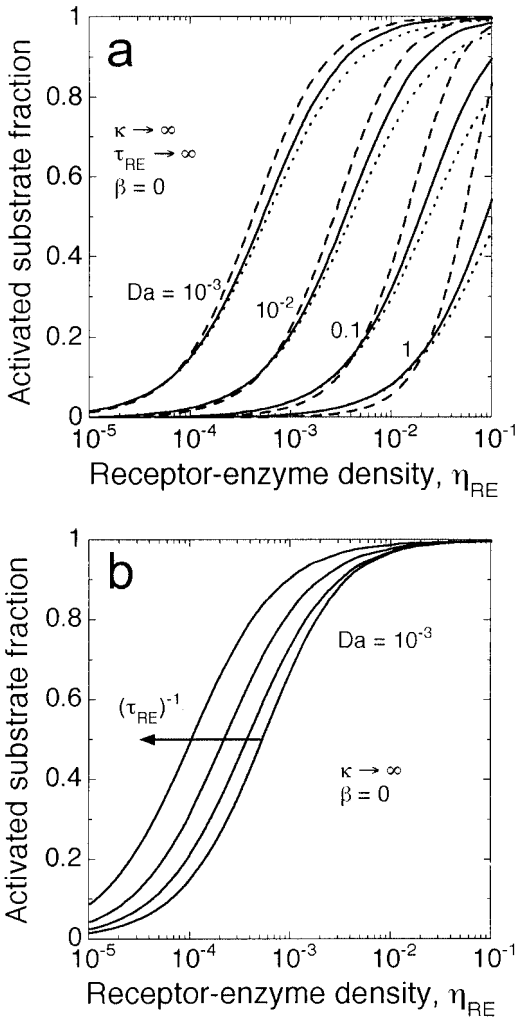

FIGURE 4 Fraction of substrate in the activated state, two-state mechanism. The activated substrate fraction is computed as a function of the receptor–enzyme density η_{RE} and constant rate parameters from Eq. 17, with $k_a = 0$ and diffusion-limited enzyme action ($\kappa \to \infty$). (*a*) Stable receptor–enzyme complexes ($\tau_{RE} \to \infty$). The value of α in Eq. 17 was calculated using: *solid lines*, the full mean field theory; *dotted lines*, the low η_{RE} limit (α constant); *dashed lines*, the MCT approach (Eq. 16). (*b*) Receptor–enzyme complexes with finite mean lifetimes. Plots are for $\eta_{RE} \ll \eta_R$, Da = 10^{-3}, and various τ_{RE} values (∞, 100, 10, and 1), with curves for lower τ_{RE} shifted to the left.

Regulated supply and turnover

Receptor-mediated substrate delivery affects the enzymatic rate constant, even when enzyme action is reaction limited

The regulated supply and turnover mechanism (Fig. 1 *b*), like the two-state mechanism, involves a receptor-recruited enzyme that acts upon a membrane-associated substrate. However, the enzymatic reaction cannot be reversed in the membrane, and so the substrate must be supplied to the membrane if steady-state signaling is to be maintained. The dynamics of the membrane lipid PI(4,5)P_2, involving the

well-characterized PLC and PI 3-kinase pathways, are well described by this pathway type. In the unstimulated cell, the constitutive rate of delivery balances basal substrate consumption; in terms of the general model, the Damköhler number, Da, is the dimensionless rate constant characterizing basal substrate turnover. Upon stimulation, activated receptors have two roles: enzyme recruitment, which increases substrate turnover, and enhanced substrate delivery. The dimensionless parameter β, absent from the two-state model, characterizes the enhancement of substrate delivery by activated receptors. To the extent that this activity affects the distribution of substrate in the membrane, it can impact the effective enzymatic rate constant.

Figure 5 shows the impact of a nonzero β value on the effective rate constant α. As in Fig. 2 *a*, α is plotted as a function of the dimensionless reaction rate constant κ in Fig. 5 *a*, in the limit of stable receptor–enzyme complexes at low density (η_R, $\eta_{RE} \to 0$, $\tau_{RE} \to \infty$). Curves are plotted for various basal turnover rates (Da = 10^{-4} – 0.1), with $\beta = 0$ or $\beta = 500$. Not surprisingly, supplying substrate in proximity to a receptor-recruited enzyme increases the effective enzymatic rate constant, an observation referred to hereafter as the β effect. At a low density of receptor–enzyme complexes, a requirement for a significant β effect is found to be βDa $\gg 1$ (Fig. 5 *a*). When Da = 10^{-4} and $\beta = 500$, α is not significantly enhanced above values for $\beta = 0$, whereas for Da = 0.1 and $\beta = 500$, α is enhanced by an order of magnitude. Thus, receptor-mediated substrate delivery spatially biases reactant consumption toward the action of receptor–enzyme complexes when the basal turnover rate is rapid. Further, Fig. 5 *a* demonstrates that this is true even in the reaction-limited regime ($\kappa < 1$), because the supply mechanism increases the substrate level near activated receptors (relative to the average concentration) under these conditions.

The influence of the activated receptor density, η_R, on the diffusion-limited effective rate constant with nonzero β is shown in Fig. 5 *b*. Curves of α versus η_R are plotted for Da values at the extremes of the range presented in Fig. 5 *a* (10^{-4} and 0.1), again with $\beta = 0$ or $\beta = 500$. Two values of η_{RE}/η_R are explored (1 and 0.1). An increase in η_R has two effects: enhancing recruitment of the enzyme, which tends to increase α in the diffusion limit, and enhancing the average substrate concentration through receptor-mediated supply, which tends to decrease α (Eq. 15). Comparing the $\beta = 0$ and $\beta = 500$ curves for Da = 10^{-4} and $\eta_{RE} = \eta_R$ in Fig. 5 *b*, a strong β effect appears at high activated receptor densities. As η_R and η_{RE} vanish, the low Da value yields a negligible β effect, whereas, at high receptor densities, α increases and tends to be independent of Da (Fig. 2 *b*), increasing the magnitude of the β effect. This synergy is strongly dependent on the value of η_{RE}/η_R; with Da = 10^{-4} and $\eta_{RE} = 0.1\eta_R$, the β effect is significantly reduced. When

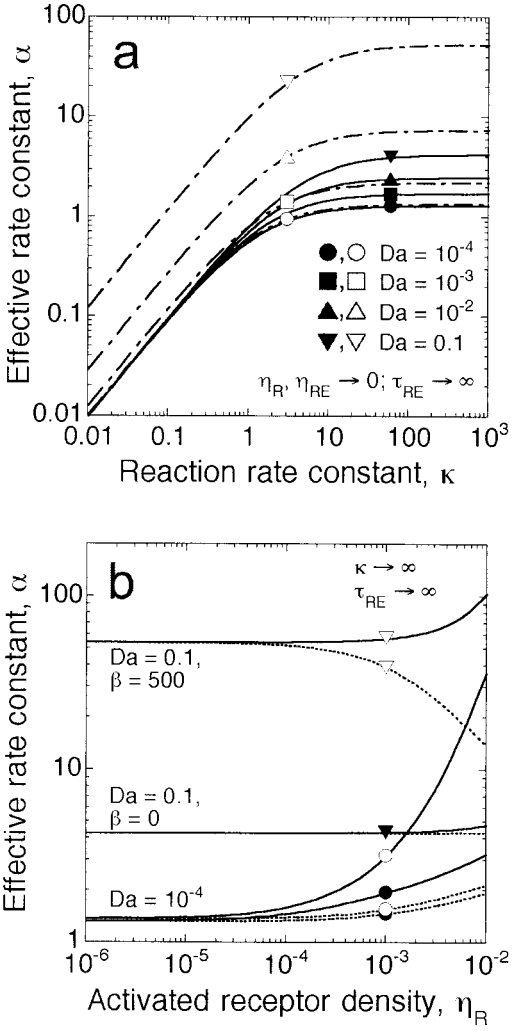

FIGURE 5 Effective enzymatic rate constant, regulated supply and turnover. In this pathway type, the dimensionless rate constant Da = $k_c s^2/D$, and the parameter β, describing receptor-mediated receptor transfer, comes into play. (*a*) The effective rate constant α is computed as a function of κ for the indicated values of Da and stable receptor–enzyme complexes at low density ($\eta_{RE} \to 0$, $\tau_{RE} \to \infty$). *Solid lines* and *closed symbols*, $\beta = 0$; *dot-dashed lines* and *open symbols*, $\beta = 500$. (*b*) The effective rate constant α is computed as a function of the dimensionless receptor–enzyme density η_{RE} for the indicated values of Da and β, diffusion-limited enzyme action, and stable receptor-enzyme complexes ($\kappa \to \infty$, $\tau_{RE} \to \infty$). *Closed symbols*, $\beta = 0$; *open symbols*, $\beta = 500$. *Solid lines*, $\eta_{RE} = \eta_R$; *dotted lines*, $\eta_{RE} = 0.1\eta_R$.

Da = 0.1, $\beta = 500$, and $\eta_{RE} = \eta_R$, the β effect is large at all densities, and so the increase in α with increasing η_R is less dramatic. When $\eta_{RE} = 0.1\eta_R$, however, a different effect is observed: the effective rate constant decreases at high η_R. Under these conditions, the major effect of an increase in η_R is an enhancement of the average substrate concentration through receptor-mediated supply. This opposes the β effect seen at low receptor activation, resulting in a merging of the $\beta = 500$ and $\beta = 0$ curves.

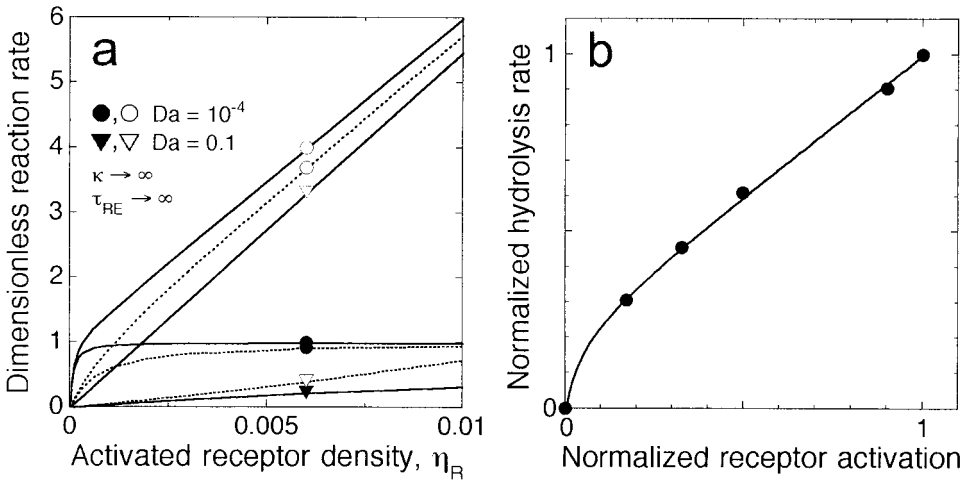

FIGURE 6 Enzymatic reaction rate, regulated supply and turnover. (*a*) Dimensionless rates of the reaction mediated by receptor–enzyme complexes are calculated from Eq. 18, for the parameter values explored in Fig. 5 *b*. *Closed symbols*, $\beta = 0$; *open symbols*, $\beta = 500$. *Solid lines*, $\eta_{RE} = \eta_R$; *dotted lines*, $\eta_{RE} = 0.1\eta_R$. Not shown are reaction rates for Da = 0.1, $\beta = 0$, and $\eta_{RE} = 0.1\eta_R$, which are linear with respect to η_R but too small to be seen on this scale. (*b*) Experimental measurements of PLC-mediated PI(4,5)P_2 hydrolysis, as a function of epidermal growth-factor receptor activation, in fibroblasts. Adapted from Haugh et al. (1999).

Prediction of enzymatic reaction rates and comparison with PI(4,5)P_2 hydrolysis data

To the extent that the regulated supply and turnover mechanism accurately depicts the action of PLC, the theory can be used to estimate the rate of PI(4,5)P_2 hydrolysis. In terms of the general model, the enzymatic reaction rate at steady state is given by

$$\frac{\text{rate}}{R_T} = \alpha\eta_{RE}\bar{\Psi}_{ss}; \quad \bar{\Psi}_{ss} = \frac{1 + \beta\eta_R}{\text{Da} + \alpha\eta_{RE}}. \qquad (18)$$

Hence, from the value of the effective rate constant α, one can compute the reaction rate as a function of η_R and compare these rates with experimental measurements of PLC-mediated PI(4,5)P_2 hydrolysis. Such a comparison is illustrated in Fig. 6.

In Fig. 6 *a*, the reaction rate is plotted versus η_R for the same parameter conditions explored in Fig. 5 *b*. When Da is low (Da = 10^{-4}), the action of the enzyme overwhelms the basal turnover rate at high η_R, such that nearly all of the substrate delivered to the membrane is consumed by the enzyme. When $\beta = 0$, the reaction rate approaches a saturated dimensionless value of one, with the enzyme reaction rate equal to the basal substrate delivery rate. The effect of receptor-mediated substrate delivery ($\beta = 500$) is to enhance this rate, and the difference between the $\beta = 500$ and $\beta = 0$ curves is proportional to η_R. Also shown in Fig. 6 *a* is the effect of enzyme recruitment on the reaction rate, with a comparison between $\eta_{RE}/\eta_R = 1$ and $\eta_{RE}/\eta_R = 0.1$. When Da = 10^{-4}, this greatly affects the magnitude of the β effect on the effective rate constant at high η_R (Fig. 5 *b*). However, because the reaction rate is determined by the substrate delivery rate under these conditions, the value of α does not significantly affect the reaction rate at high η_R.

When Da is relatively high (Da = 0.1), basal turnover remains the dominant mode of substrate consumption for the range of η_R shown. Here, enzymatic reaction rates are more or less proportional to η_R (Fig. 6 *a*), but it is not immediately apparent how the slopes of these lines depend on the constant parameters. With Da = 0.1 and $\beta = 500$, receptor-mediated substrate delivery significantly enhances both the average substrate concentration and the effective rate constant α (Fig. 5). In fact, when Eqs. 15 and 18 are compared, it is clear that, for higher Da and βDa $\gg 1$, the enzymatic reaction rate is completely independent of the average substrate concentration. The receptor-mediated supply mechanism creates a small zone of substrate around the receptor, and the enzymatic reaction rate approaches $\beta\eta_{RE}$ (Fig. 6 *a*; Da = 0.1, $\beta = 500$ curves).

How do the shapes of the reaction rate versus receptor activation curves compare with experiment? Figure 6 *b* shows measurements of PLC-mediated PI(4,5)P_2 hydrolysis rates as a function of epidermal growth factor receptor activation in fibroblasts (Haugh et al., 1999). These results were obtained using a cell line with $\sim 4 \times 10^5$ receptors per cell; this yields a maximum η_R value of $\sim$0.01, corresponding to the range shown in Fig. 6 *a*. The data in Fig. 6 *b* are clearly similar to the low Da, nonzero β curves shown in Fig. 6 *a*. In accord with a previous theoretical study that did not account for substrate diffusion (Haugh et al., 2000), it is concluded that low (but nonzero) basal turnover rates and enhancement of substrate supply are required to match observations. Further, because diffusion-limited rates are shown in Fig. 6 *a*, it is concluded that Da = 10^{-4} is at the

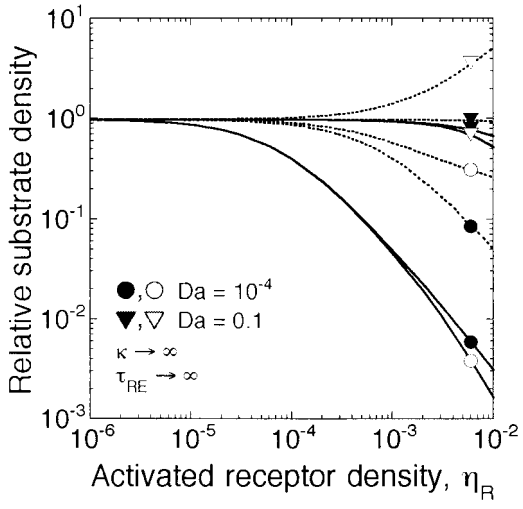

FIGURE 7 Average substrate concentration, regulated supply and turnover. The dimensionless average concentration of the substrate at steady-state $\bar{\Psi}_{ss}$, normalized by its basal value (1/Da), is plotted versus receptor activation η_R for the parameter values explored in Figs. 5 *b* and 6 *a*. *Closed symbols*, $\beta = 0$; *open symbols*, $\beta = 500$. *Solid lines*, $\eta_{RE} = \eta_R$; *dotted lines*, $\eta_{RE} = 0.1\eta_R$.

high end of the range that will mimic Fig. 6 *b*. This is consistent with experiments in other cell systems. Willars et al. (1998) measured a basal PI(4,5)P_2 turnover-time constant of ~300 s in neuroblastoma cells, whereas the time constant during stimulation with carbachol at steady state is ~5 s; with a diffusion coefficient of ~0.5 $\mu m^2/s$, a Da value of ~10^{-7} is obtained. As mentioned previously, the enhancement of substrate supply is also supported by experimental evidence. Indeed, Willars et al. also showed that the carbachol-sensitive pool of PI(4,5)P_2 decreases to ~13% of its initial level following stimulation, despite the 60-fold increase in the PI(4,5)P_2 consumption rate. This implies a nearly 8-fold increase in substrate supply.

The average substrate concentration at steady state can be enhanced or diminished by receptor-mediated substrate delivery

As demonstrated in Fig. 6 *a*, the rate of the reaction catalyzed by the receptor-recruited enzyme does not depend on the effective enzymatic rate constant when basal turnover (Da) is relatively low. However, under these conditions, the effective rate constant has a significant impact on the steady-state substrate level; in the case of the PLC pathway, modulation of the PI(4,5)P_2 concentration can influence the action of PI 3-kinases and other pathways. Further, because receptor-mediated substrate delivery can affect the enzymatic rate constant (Fig. 5), enhanced substrate delivery may not necessarily yield an increase in the substrate level.

Figure 7 shows the predicted dependence of the average, steady-state substrate density on receptor activation (η_R), for the parameter conditions explored in Figs. 5 *b* and 6 *a*. An analysis of Eq. 15 shows that receptor-mediated substrate supply enhances the average substrate concentration (relative to $\beta = 0$) if either the β effect on α is small or η_{RE} is not very close to η_R ($\eta_{RE} = 0.1\eta_R$ curves, Fig. 7). Further analysis demonstrates that the β effect on α must be small if this enhancement is to be significant. In contrast, for both Da values (10^{-4} and 0.1), substrate concentrations for $\beta = 500$ are actually reduced relative to the values for $\beta = 0$ when $\eta_{RE} = \eta_R$. How can receptor-mediated substrate delivery enhance depletion of the substrate? Whereas substrate delivery depends linearly on η_R for nonzero β, the effective enzymatic rate constant is a nonlinear function of η_R and, by extension, η_{RE} (Eq. 15). This sensitive dependence at higher η_{RE} arises from the overlap of substrate depletion zones surrounding neighboring receptor–enzyme complexes. When $\eta_{RE} \approx \eta_R$, the β effect on α causes this overlap to occur at lower η_R, such that substrate depletion is enhanced more than the increase in substrate supply.

The possibility that receptor-mediated substrate supply could reduce the level of PI(4,5)P_2 is inconsistent with experimental evidence; as discussed previously, the decrease in PI(4,5)P_2 observed in stimulated cells is typically much less drastic than the level predicted from the change in turnover rate. It is therefore unlikely that β strongly influences the effective PLC rate constant. Further, if PLC action is diffusion-limited and Da is low, it is predicted that η_{RE}/η_R must be ~0.1 or less for α to be largely independent of β (Fig. 5 *b* and calculations not shown).

Potential modifications to the theory and other applications

The ability to analyze distinct signaling pathways with very different modes of substrate regulation underscores the versatility of the general model. In addition, more complex mechanisms can be included in the model with minor modifications. For example, one could account for competing enzyme activities that independently engage signaling receptors, such as the consumption of PI(4,5)P_2 by PLC and PI 3-kinase activities. To accomplish this, one would need to separately account for activated receptor pools bound to one, the other, or both enzymes, with a distinct boundary condition for each. The substrate conservation equation would then include the sum of these activities in the mean field. This approach can also be applied to a receptor able to engage more than one molecule of the same enzyme (e.g., oligimerized receptor complexes), and to multiple receptor types that bind common enzymes. Another possible variation of the model involves receptor control of enzymes that oppose

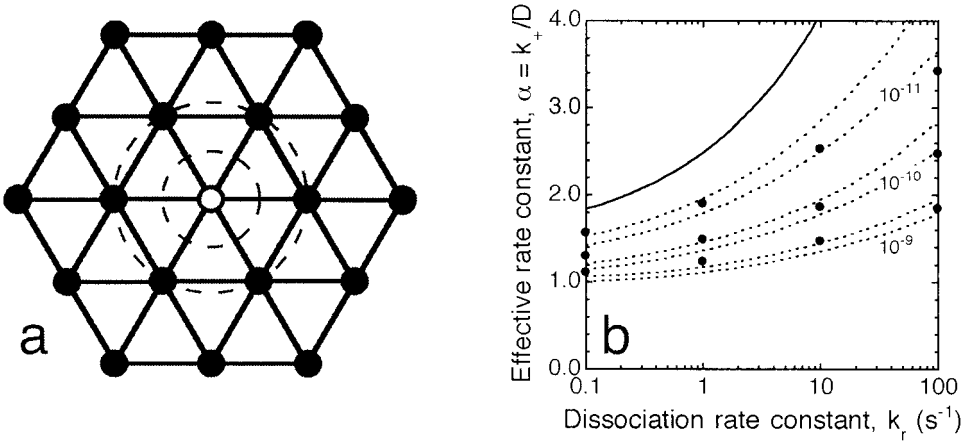

FIGURE A1 Comparison of the mean field theory and Monte Carlo simulations for the collision coupling mechanism. (*a*) Intermolecular interactions on a lattice. As described in the text, the encounter distance *s* is half of the lattice spacing *l*; these two distances from the absorber are denoted by the dashed circles. Simulating point particles on a lattice cannot resolve concentrations gradients with a resolution less than *l*. (*b*) Numerical comparison. Constant parameters are $k_i = 0.1\ s^{-1}$, $n_{R,tot} = 40\ \mu m^{-2}$, $s = 3.5$ nm, and $[L]/K_D = 0.05$, yielding $\eta_{RE} = \eta_R = 2.333 \times 10^{-5}$. Species diffusion coefficients (D/2) are 10^{-9}, 10^{-10}, and $10^{-11}\ cm^2/s$, yielding Da values of 6.125×10^{-6}, 6.125×10^{-5}, and 6.125×10^{-4}, respectively. The dimensionless complex lifetime $\tau_{RE} = (D/s^2)/k_r$, where k_r is the ligand dissociation rate constant. To account for the spatially discrete nature of a lattice, a finite value of κ is used in the mean field theory to directly compare the two methods. Plotted are values of α calculated for the parameters listed above, with D/2 values in cm^2/s as indicated, as a function of k_r. The appropriate bounds are $\kappa = 2\pi$ and $\kappa = 2\pi/\ln(2)$ (*dotted lines*), with the latter yielding the higher α values. Also plotted is the diffusion-limited curve (κ approaching infinity) for $D/2 = 10^{-11}\ cm^2/s$ (*solid line*). Circle symbols are Monte Carlo simulation results adapted from Shea et al. (1997).

each other's action (e.g., GEFs/GAPs). This can be incorporated in a similar fashion to the competitive enzyme variation just described, with modifications to reflect the fact that the enzymes act on different substrates. Finally, the theory can be modified to consider finite domain sizes, which could be used to mimic the effect of lipid microdomains. These low-density lipid assemblies, which can be regulated by cytoskeletal interactions, are thought to impact the compartmentalization and mobility of many membrane-associated signaling molecules (Mineo et al., 1996; Pike and Casey, 1996; Pralle et al., 2000).

Spatial considerations have been largely overlooked in mathematical models of signaling processes, particularly in models of considerable scope (Weng et al., 1999). The generality of the analytical model presented here suggests that it could be embedded within broader models of receptor-mediated signal-transduction networks. With such a modular approach (Asthagiri and Lauffenburger, 2000), smaller models could swap information if the dynamics affecting input variables (e.g., the density of receptor–enzyme complexes) are considerably slower than the processes within the module. Indeed, it has previously been noted that receptor–ligand binding and trafficking processes are probably slow compared to enzyme recruitment and other early signaling events (Haugh and Lauffenburger, 1997, 1998). A modular strategy would enable modeling of feedback and crosstalk among multiple parallel pathways, significantly expanding the predictive capability of signaling models and enhancing our ability to manipulate cell function.

APPENDIX

Quantitative comparison of the mean field, continuum theory with Monte Carlo simulations on a lattice

The diffusion-limited collision-coupling activation mechanism in membranes was examined by Shea et al. (1997), using Monte Carlo simulations of point particles on a lattice. This mechanism is indistinguishable from the two-state mechanism illustrated in Fig. 1 *a*, with $k_a = 0$. The receptor–enzyme complex is simply an activated receptor in this case ($\eta_{RE} = \eta_R$), and η_R is calculated from the extracellular ligand concentration [L]: $\eta_R = \eta_{R,tot}[L]/(K_D + [L])$, where $\eta_{R,tot}$ is the value of η_R when all receptors are activated, and K_D is the dissociation constant of the ligand–receptor interaction. Finally, the lifetime τ_{RE} is redefined as the average lifetime of a ligand–receptor complex: $\tau_{RE} = (D/s^2)/k_r$, where k_r is the first-order ligand dissociation (reverse) rate constant. Thus, it is possible to directly compare the analytical results obtained from the mean field model to the Monte Carlo simulations performed by Shea and colleagues.

First, a technical note on lattice representations of 2D surfaces is in order. Shea et al. used a triangular lattice, with discrete particles occupying single points. The lattice spacing *l* and the number of simulation steps were scaled to distance ($l = 7$ nm) and time, respectively. Movement (diffusion) of the particles to adjacent lattice points occurs randomly, and particles are not allowed to occupy the same node. An activation step occurs when activated receptor and inactive substrate molecules want to move to the same point; the substrate particle is reassigned as "activated" and placed one lattice point away from the receptor. Thus, in one diffusion step, the particles effectively move a half jump toward each other, then a half jump away. The encounter distance *s* is therefore *l*/2 (Fig. A1 *a*). When the lifetime of the activated receptor is very short, Shea et al. showed that the probability density profile of inactive substrate surrounding each activated receptor tends toward homogeneity, increasing the diffusion-limited activation rate constant. This

implies that the gradient of inactive substrate very close to an activated receptor particle gets large as k_r gets large. However, for point particles on a lattice, this gradient cannot be described at a resolution less than l, resulting in an underestimation of the effective rate constant.

In contrast, analytical models such as the mean field theory treat the membrane as a continuum, such that the inactive substrate gradient can be arbitrarily large. How, then, can lattice and continuum models be compared? An approximate method is suggested by the boundary condition for the continuum model at the encounter distance s:

$$2\pi s \frac{\partial n_S}{\partial r}\bigg|_{r=s} = \kappa n_S|_{r=s}, \qquad \text{(A1)}$$

where n_S is the concentration of the inactive substrate, and κ is a second-order reaction rate constant, scaled by the diffusion coefficient D. In the translational diffusion limit, κ approaches infinity. However, the effective gradient, represented on the left side of Eq. A1, is limited in value for a lattice model. This suggests that the continuum model can be compared to the lattice model results by using a finite κ value on the right side of Eq. A1.

Approaching the limit of infinite k_r in the lattice model, the inactive substrate concentration at a distance $l = 2s$ from an activated receptor particle will approach the average concentration $\bar{n}_S$. In a triangular lattice, inactive substrate particles can encounter an activated receptor via six paths (Fig. A1 *a*). If this number were reduced to one, Laplace's equation could be solved in one dimension (1D) to derive the effective profile between $r = s$ ($n_S = 0$) and $r = 2s$ ($n_S \approx \bar{n}_S$). The result, of course, is a straight line. Substituting into Eq. A1,

$$2\pi s \frac{\partial n_S}{\partial r}\bigg|_{r=s} = 2\pi s\left(\frac{\bar{n}_S - 0}{2s - s}\right) = \kappa \bar{n}_S \quad \text{(1D)}. \qquad \text{(A2)}$$

It follows that the minimum value for κ is 2π. On the other extreme, if the number of paths to an activated receptor were increased from six to infinity, one could solve for the radial profile in 2D. It is readily shown that this yields a κ value of $2\pi/\ln(2)$.

Figure A1 *b* shows that values of the dimensionless effective rate constant α, calculated using Eq. 14 with κ in the range of 2π to $2\pi/\ln(2)$, are in excellent numerical agreement with values obtained by Shea et al. It should be noted that a modest error is introduced due to the inexactness of Eq. 14, which assumes very long periods between enzyme–receptor associations. The consequence of a shorter τ_R is that $\Psi(\sigma, 0)$ for the ligand-on phase will tend to be less than $\bar{\Psi}$, resulting in a reduced effective rate constant. However, even for the lowest τ_R value in Fig. A1 *b* ($D/2 = 10^{-11}$ cm^2/s, $k_r = 100$ s^{-1}), accounting for this deviation by simulating successive enzyme on/off cycles yielded an α value only ~2% below that predicted by Eq. 14. Figure A1 *b* also demonstrates that the Monte Carlo simulation results deviate significantly from diffusion-limited values calculated using the continuum model ($\kappa \to \infty$). This derives from the treatment of molecules as point particles, which limits the spatial resolution of the simulation, and the discrepancy is predictably an increasing function of k_r. With that said, it is fully expected that lattice simulations would approach an exact result as particles are allowed to fill an increasing number of lattice points, allowing a true test of the continuum model to be performed.

The author gratefully acknowledges Lonnie Shea (Dept. of Chemical Engineering, Northwestern University) and Jennifer Linderman (Dept. of Chemical Engineering, University of Michigan) for helpful discussions regarding Monte Carlo simulations on lattices, and for providing numerical results from their previous work.

REFERENCES

Adam, G., and M. Delbrück. 1968. Reduction of dimensionality in biological diffusion processes. *In* Structural Chemistry and Molecular Biology. W. H. Freeman and Co., San Francisco. A. Rich and N. Davidson, editors. 198–215.

Aronheim, A., D. Engelberg, N. Li, N. Al-Alawi, J. Schlessinger, and M. Karin. 1994. Membrane targeting of the nucleotide exchange factor Sos is sufficient for activating the Ras signaling pathway. *Cell.* 78:949–961.

Asthagiri, A. R., and D. A. Lauffenburger. 2000. Bioengineering models of cell signaling. *Annu. Rev. Biomed. Eng.* 2:31–53.

Batty, I. H., R. A. Currie, and C. P. Downes. 1998. Evidence for a model of integrated inositol phospholipid pools implies an essential role for lipid transport in the maintenance of receptor-mediated phospholipase C activity in 1321N1 cells. *Biochem. J.* 330:1069–1077.

Berg, H. C., and E. M. Purcell. 1977. Physics of chemoreception. *Biophys. J.* 20:193–219.

Buday, L., and J. Downward. 1993. Epidermal growth factor regulates $p21^{ras}$ through the formation of a complex of receptor, Grb2 adapter protein, and Sos nucleotide exchange factor. *Cell.* 73:611–620.

Carslaw, H. S., and J. C. Jaeger. 1940. Some two-dimensional problems in conduction of heat with circular symmetry. *Proc. Lond. Math. Soc. (2).* 46:361–388.

Dodd, T. L., D. A. Hammer, A. S. Sangani, and D. L. Koch. 1995. Numerical simulations of the effect of hydrodynamic interactions on diffusivities of integral membrane-proteins. *J. Fluid Mech.* 293: 147–180.

Feder, T. J., I. Brust-Mascher, J. P. Slattery, B. Baird, and W. W. Webb. 1996. Constrained diffusion or immobile fraction on cell surfaces: a new interpretation. *Biophys. J.* 70:2767–2773.

Freeman, D. L., and J. D. Doll. 1983. The influence of diffusion on surface reaction kinetics. *J. Chem. Phys.* 78:6002–6009.

Goldstein, B., C. Wofsy, and H. Echavarria-Heras. 1988. Effect of membrane flow on the capture of receptors by coated pits: theoretical results. *Biophys. J.* 53:405–414.

Hamm, H. E., and A. Gilchrist. 1996. Heterotrimeric G proteins. *Curr. Opin. Cell Biol.* 8:189–196.

Haugh, J. M., and D. A. Lauffenburger. 1997. Physical modulation of intracellular signaling processes by locational regulation. *Biophys. J.* 72:2014–2031.

Haugh, J. M., and D. A. Lauffenburger. 1998. Analysis of receptor internalization as a mechanism for modulating signal transduction. *J. Theor. Biol.* 195:187–218.

Haugh, J. M., K. Schooler, A. Wells, H. S. Wiley, and D. A. Lauffenburger. 1999. Effect of epidermal growth factor receptor internalization on regulation of the phospholipase C-γ1 signaling pathway. *J. Biol. Chem.* 274:8958–8965.

Haugh, J. M., A. Wells, and D. A. Lauffenburger. 2000. Mathematical modeling of epidermal growth factor receptor signaling through the phospholipase C pathway: mechanistic insights and predictions for molecular interventions. *Biotech. Bioeng.* 70:225–238.

Howells, I. D. 1974. Drag due to motion of a Newtonian fluid through a sparse random array of small fixed rigid objects. *J. Fluid Mech.* 64: 449–475.

Hsuan, J. J., and S. K. Tan. 1997. Growth factor-dependent phosphoinositide signalling. *Int. J. Biochem. Cell Biol.* 29:415–435.

Kauffmann-Zeh, A., R. Klinger, G. Endemann, M. D. Waterfield, R. Wetzker, and J. J. Hsuan. 1994. Regulation of human type II phosphatidylinositol kinase activity by epidermal growth factor-dependent phosphorylation and receptor association. *J. Biol. Chem.* 269:31243–31251.

Kauffmann-Zeh, A., G. M. H. Thomas, A. Ball, S. Prosser, E. Cunningham, S. Cockcroft, and J. J. Hsuan. 1995. Requirement for phosphatidylinositol transfer protein in epidermal growth factor receptor signaling. *Science.* 268:1188–1190.

Keizer, J., J. Ramirez, and E. Peacock-Lopez. 1985. The effect of diffusion on the binding of membrane-bound receptors to coated pits. *Biophys. J.* 47:79–88.

Khakhar, D. V., and U. S. Agarwal. 1993. Competition effects in surface diffusion-controlled reactions: theory and Brownian dynamics simulations. *J. Chem. Phys.* 99:9237–9247.

Kholodenko, B. N., J. B. Hoek, and H. V. Westerhoff. 2000. Why cytoplasmic signalling proteins should be recruited to cell membranes. *Trends Cell Biol.* 10:173–178.

Klippel, A., C. Reinhard, W. M. Kavanaugh, G. Apell, M. Escobedo, and L. T. Williams. 1996. Membrane localization of phosphatidylinositol 3-kinase is sufficient to activate multiple signal-transducing kinase pathways. *Mol. Cell. Biol.* 16:4117–4127.

Lenzen, C., R. H. Cool, H. Prinz, J. Kuhlmann, and A. Wittinghofer. 1998. Kinetic analysis by fluorescence of the interaction between Ras and the catalytic domain of the guanine nucleotide exchange factor $Cdc25^{Mm}$. *Biochemistry.* 37:7420–7430.

Mahama, P. A., and J. L. Linderman. 1994. A Monte Carlo study of the dynamics of G-protein activation. *Biophys. J.* 67:1345–1357.

Medema, R. H., A. M. M. De Vries-Smits, G. C. M. Zon, J. A. Maassen, and J. L. Bos. 1993. Ras activation by insulin and epidermal growth factor through enhanced exchange of guanine nucleotides on $p21^{ras}$. *Mol. Cell. Biol.* 13:155–162.

Mineo, C., G. L. James, E. J. Smart, and R. G. W. Anderson. 1996. Localization of epidermal growth factor-stimulated Ras/Raf-1 interaction to caveolae membrane. *J. Biol. Chem.* 271:11930–11935.

Molski, A. 2000. A model of diffusion-influenced enzyme activation. *J. Phys. Chem. B.* 104:4532–4536.

Niv, H., O. Gutman, Y. I. Henis, and Y. Kloog. 1999. Membrane interactions of a constitutively active GFP-Ki-Ras 4B and their role in signaling. *J. Biol. Chem.* 274:1606–1613.

Pawson, T. 1995. Protein modules and signaling networks. *Nature.* 373: 573–580.

Pike, L. J., and L. Casey. 1996. Localization and turnover of phosphatidylinositol 4,5-bisphosphate in caveolin-enriched membrane domains. *J. Biol. Chem.* 271:26453–26456.

Pralle, A., P. Keller, E.-L. Florin, K. Simons, and J. K. H. Hörber. 2000. Sphingolipid-cholesterol rafts diffuse as small entities in the plasma membrane of mammalian cells. *J. Cell Biol.* 148:997–1007.

Quilliam, L. A., S. Y. Huff, K. M. Rabun, W. Wei, W. Park, D. Broek, and C. J. Der. 1994. Membrane-targeting potentiates guanine nucleotide exchange factor Cdc25 and Sos1 activation of Ras transforming activity. *Proc. Natl. Acad. Sci. U.S.A.* 91:8512–8516.

Rameh, L. E., and L. C. Cantley. 1999. The role of phosphoinositide 3-kinase lipid products in cell function. *J. Biol. Chem.* 274:8347–8350.

Rhee, S. G., and Y. S. Bae. 1997. Regulation of phosphoinositide-specific phospholipase C isozymes. *J. Biol. Chem.* 272:15045–15048.

Schlessinger, J., D. Axelrod, D. E. Koppel, W. W. Webb, and E. L. Elson. 1977. Lateral transport of a lipid probe and labeled proteins on a cell membrane. *Science.* 195:307–309.

Shea, L. D., G. M. Omann, and J. J. Linderman. 1997. Calculation of diffusion-limited kinetics for the reactions in collision coupling and receptor cross-linking. *Biophys. J.* 73:2949–2959.

Sheetz, M. P. 1993. Glycoprotein motility and dynamic domains in fluid plasma membranes. *Annu. Rev. Biophys. Biomol. Struct.* 22:417–431.

Toker, A. 1998. The synthesis and cellular roles of phosphatidylinositol 4,5-bisphosphate. *Curr. Opin. Cell Biol.* 10:254–261.

Tolkovsky, A. M., and A. Levitski. 1978. Mode of coupling between the β-adrenergic receptor and adenylate cyclase in turkey erythrocytes. *Biochemistry.* 17:3795–3810.

van der Geer, P., T. Hunter, and R. A. Lindberg. 1994. Receptor protein-tyrosine kinases and their signal transduction pathways. *Annu. Rev. Cell Biol.* 10:251–337.

Vanhaesebroeck, B., and M. D. Waterfield. 1999. Signaling by distinct classes of phosphoinositide 3-kinases. *Exp. Cell Res.* 253:239–254.

Weng, G., U. S. Bhalla, and R. Iyengar. 1999. Complexity in biological signaling systems. *Science.* 284:92–96.

Wiegel, F. W., and C. DeLisi. 1982. Evaluation of reaction rate enhancement by reduction in dimensionality. *Am. J. Physiol. Regulatory Integrative Comp. Physiol.* 12:R475–R479.

Willars, G. B., S. R. Nahorski, and R. A. J. Challiss. 1998. Differential regulation of muscarinic acetylcholine receptor-sensitive polyphosphoinositide pools and consequences for signaling in human neuroblastoma cells. *J. Biol. Chem.* 273:5037–5046.

Wittinghofer, A. 1998. Signal transduction via Ras. *Biol. Chem.* 379: 933–937.

Wittinghofer, A., K. Scheffzek, and M. R. Ahmadian. 1997. The interaction of Ras with GTPase-activating proteins. *FEBS Lett.* 410:63–67.